Excited State Relaxation Dynamics of Silicon Nanosheets using Time-dependent Density Functional Tight Binding Theory

M Y Wang[1] and Q Wu[1,2*]

1 School of Science, Tibet University, Lhasa City, 850000, China
2 School of Environmental Science and Engineering, Tianjin University, Tianjin, 300072, China
Email: wuqi_zangda@163.com

Abstract. By combining time-dependent density functional tight binding (TD-DFTB) calculations for electrons with molecular dynamics simulations, time evolution of excited state relaxation and single electron self-trapping of silicon nanosheets (Si_nH_m) are investigated. We identify the atoms and bonds contributing to the excitations and observe the time evolution of charge density, indicating the migration of exciton from initial position to neighboring bonds. Different temperature 50K and 100K are attempted in the MD simulations, and the temperature is found to affect the electronic localization. Our simulations reveal the formation of exciton trapping and localization on certain bonds upon excitation within the timescale about 200-300fs. In summary, TD-DFTB excited state MD simulations can provide interesting insights into photoreactions and have crucial implications in modulating the exciton transport efficiency in strongly confined low-dimensional systems.

1. Introduction

Electronically excited states play a prominent role in many different areas of chemical and condensed matter physics and organic chemistry [1-2]. For example, luminescence energies and the resonance Raman spectra are associated with the displacement of the geometry in the excited state. The fluorescent properties of excited state systems are increasingly being employed as biomolecular probes [3-4]. Despite their obvious importance, a detailed investigation of the excited state remains a challenge to experimentalists and theoreticians alike. The interpretation of emission spectra is complicated by the fact that a detailed configurational representation of the experimental data requires knowledge of both the excited state and ground state energy surfaces [5].

Linear response time-dependent density functional theory (TD-DFT) based on Casida's equations [6] is probably the most widely used method for the simulation of processes involving excited states, such as photon absorption and emission [7-8]. Its success is due to the relatively modest numerical efficiency combined with the generally good level of accuracy. However, although the TD-DFT is much cheaper in terms of computational cost, simulations of nanosystems with hundreds of atoms are still out of reach. Hence, there is a clear need for computationally inexpensive electronic structure theory methods which can model the excited state potential energy surfaces. Based on the framework of the density functional based tight binding (DFTB) [9-10], a computationally very efficient alternative to TD-DFT has been developed in the form of time-dependent DFTB [11-12]. The time-dependent density functional tight binding (TD-DFTB) developed by T. A. Niehaus become widely used for the calculation of the vertical excitation energies and excited state properties of medium- to

large-size molecular systems [13-21]. It has been shown that TD-DFTB yields reasonable agreement for optical spectra with experiments and first-principles calculations at a highly reduced cost in many cases.

However current TD-DFTB theory could only provide static excited state calculations, which is not efficient as dynamic information is totally lost. Photochemical reactions typically occur at femto- to picosecond timescales. As the relevant time and spatial resolutions are hard to access in experiment, molecular dynamics simulation is the best method of choice to study such ultrafast processes and resolve. Therefore, excited state molecular dynamic simulations are currently one of the frontiers of computational chemistry. These simulations demand a delicate combination of high-quality and high-speed methods to achieve a proper description of the excited-state time evolution of molecules. By combining time-dependent density functional tight binding (TD-DFTB) calculations for electrons with molecular dynamics simulations, here we investigate the capability of time-dependent density functional tight binding method to describe the time evolution of excited state potential energy surfaces. This yields the possibility of studying the trajectory following photo-excitation and of identifying the most important degree of freedoms involved in the excited state relaxation.

2. Methodology and model description

2.1. Time-dependent density functional tight binding theory

For a given structure, the total energy for an excited state is obtained in two steps. A self-consistent field (SCF) calculation is first conducted to obtain the single particle Kohn-Sham (KS) orbitals ψ_i and the corresponding KS energies ε_i. These single particle results are then corrected following TD-DFT linear response treatment of Casida6 错误!未定义书签。.

$$\sum_{kl\tau}[\omega_{ij}^2\delta_{jl}\delta_{\sigma\tau} + 2\sqrt{\omega_{ij}}K_{ij\sigma,kl\tau}\sqrt{\omega_{kl}}]F_{kl\tau}^I = \omega_I^2 F_{ji\sigma}^I \tag{1}$$

Where $\omega_{ij} = \varepsilon_j - \varepsilon_i$ and σ, τ are spin indices.

The coupling matrix is obtained by giving the SCF potential with respect to the electronic density change as follows:

$$K_{ij\sigma,kl\tau} = \iint \psi_i(\mathbf{r})\psi_j(\mathbf{r})(\frac{1}{|\mathbf{r}-\mathbf{r}'|} + \frac{\delta^2 E_{xc}}{\delta\rho_\sigma(\mathbf{r})\delta\rho_\tau(\mathbf{r}')})\psi_k(\mathbf{r}')\psi_l(\mathbf{r}')d\mathbf{r}d\mathbf{r}' \tag{2}$$

Equation (2) is further simplified in TD-DFTB approach using the Mulliken approximation [22-23].

From the results of Equation (1), oscillator strengths for singlet-singlet transitions are calculated according to Eq. (3):

$$f_I = \frac{2}{3}\omega_I\sum_{k=x,y,z}\left|\sum_{ij}\langle\psi_i|\mathbf{r}_k|\psi_j\rangle\sqrt{\frac{\omega_{ij}}{\omega_I}}(F_{ij\uparrow}^I + F_{ij\downarrow}^I)]\right|^2 \tag{3}$$

By solving the energies and oscillator strengths of ten lowest singlet excitations, we obtained the low energy part of the absorption spectrum for the ground state (S_0). Finally, the emission energies are evaluated by geometry optimization in the first excited singlet state (S_1), based on the assumption of rapid internal conversion, (i.e., the validity of Kasha's rule).

2.2 Molecular dynamics simulation

Our TD-DFTB molecular dynamics are purely adiabatic and proceed in the following way. The nuclear time evolution is treated classically by means of the Newton's equations, while the population of each electronic state is treated separately.

First, a simulation in S_0 is carried out in order to obtain an equilibrated system at the target temperature using a Berendsen thermostat. We then take random configurations (coordinates and velocities) from this simulation and vertically excite the system into a selected singlet state. The positions of the nuclei are updated according to the forces computed as the gradients of the excited state energy. In a second iteration, the excited state density and Kohn-Sham orbitals for the latest geometry are computed, and the TD-DFTB calculation provides the new excited state energy and the new forces on the nuclear. This approach allows us to adiabatically follow the instantaneous electronic excited state PES in the Born-Oppenheimer molecular dynamic scheme.

2.3 Application of TD-DFTB molecular dynamics simulations to silicon nanosheets

We reported the theoretical prediction of excited state relaxation and single electron self-trapping in Si nanosheets. In finite atomic cluster, we show that excitons are strongly localized around the Si-Si dimer with the bond distance enlarged. Analysis of molecular orbitals in the excited state exhibits a localized distribution along the distorted areas of the Si nanosheets. While a static exploration of the geometry provides only an incomplete study of relaxation on the excited state surface, molecular dynamics (MD) simulation is thus available for an understanding and confirmation of excited state relaxation at different temperature were thus carried out for S_1 state.

As an extension of our previous work on the effect of the edge width on exciton distribution in two-dimensional nanosheets, we herein explored the excited state relaxation of the most widely investigated Si (110) [24-27] oriented nanosheets using TD-DFTB molecular dynamic simulations. Detailed information about the computational model can be found in ref 20 . Due to restrictions in computational power, the excited state molecular dynamic simulations are only performed for Si sheets ($Si_{30}H_{48,}$ $Si_{60}H_{82}$ and $Si_{90}H_{116}$). In order to examine the temperature effect on the excited state relaxation, MD simulations at 50K and 100K were attempted for each structure respectively.

The performance of TD-DFTB [28-31] against TD-DFT [12,32] has been characterized by many groups. For instance, the optical gap of Si_5H_{12} cluster was predicted as 6.4 eV [15], close to the experimental value of 6.5 eV [33]. For other larger clusters like $Si_{35}H_{36}$, the absorption energies (4.37eV) calculated using TD-DFTB coincides with the results (4.33 eV [34]) obtained using a high level *ab initio* multi-reference second order Møller–Plesset perturbation theory (MR-MP2). Meng *et al*. [35] also confirmed the reliability of TD-DFTB by comparing the calculated absorption energies with the results using PBE, which exhibits that the difference in absorption energies is only around 0.1eV. In general, these comparisons confirm that TD-DFTB offers acceptable accuracy to investigate the excited state properties of the hydrogenated silicon nanoparticles, and enables our study to be extended from several atoms to nanometer-size systems.

3. Results and discussion

3.1 MD simulation in S_1 state for $Si_{30}H_{48}$ at 50K and 100K

MD simulations in S_1 state of $Si_{30}H_{48}$ were performed at 50K and 100K, respectively. As Figure 1(a) shows, vital Si-Si bonds were labeled clearly to exhibit the excited state relaxation. The time evolution of bond length change of several Si-Si dimer are also shown in Figure 1(b). We observe that the Si-Si bond 2 extends to 2.79 Å at 82.5fs and exhibit an average bond length about 2.8 Å, which is consistent with our static calculation of the excited state (see Figure 5.3 in ref 20). While the other Si-Si bonds, for instance, bonds 2, 3, 4 and 5 in the vicinity remain almost unchanged. It is determined that the exciton is firstly localized on Si-Si bond 2. With the simulation time increases to 480fs, bond 2 exhibits an abrupt decrease in length and bond 3 becomes elongated, accordingly. The exciton is hence localized on bond 2 and bond 3.
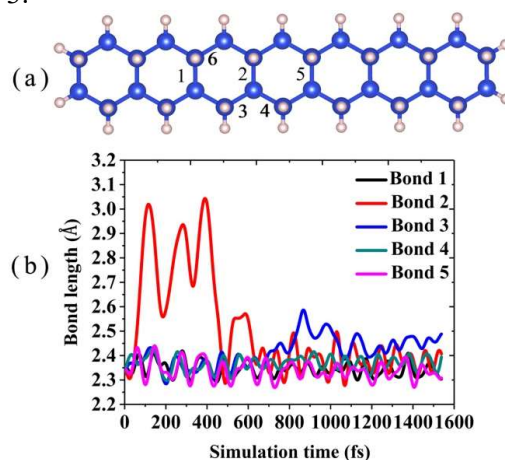

Figure 1. The structures of (a) SiNS $Si_{30}H_{48}$ and (b) time evolution of bond length change of labeled bonds at 50K. Si and H atoms are shown as blue and white balls, respectively. The numbers show the labeling of vital bonds of the SiNS.

To further interpret the optical properties of SiNSs, the LUMO (defined as the orbital which is occupied by one excited electron) in the S_1 state are plotted in Figure 2. Figure 2 (a) shows the non-localized distribution of LUMO in the vertical excite state of $Si_{30}H_{48}$. In the beginning of excitation, the LUMO in S_1 is distributed on several central Si bonds. In contrast, the molecular orbital of the structures at 115.5fs indicates a localized distribution and also a trapped exciton on the Si-Si bond. More interestingly, it is observed that the localization is not fixed on bond 2 anymore. With the elongation of bond 3, the trapped exciton has a shift in distribution when the simulation time is longer than 870fs, indicating the migration of electron from initial position to neighboring bonds. It is thus determined that the MD simulations in S_1 state yields reasonable forces and a reliable description of excited state relaxation compared with our static excited state calculations .
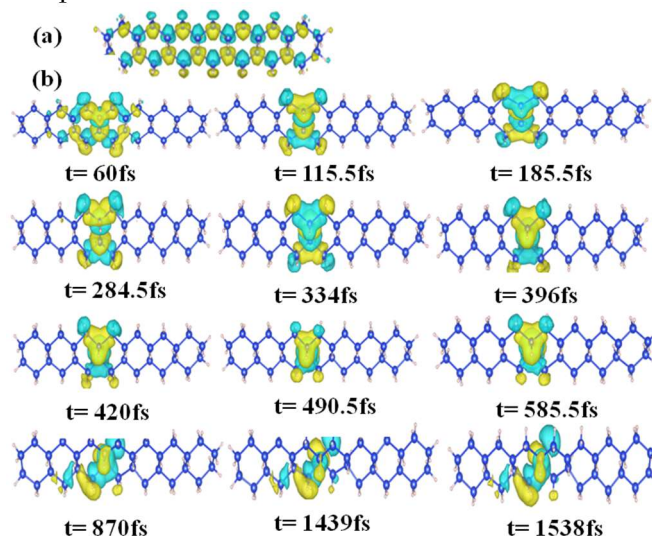

Figure 2. Frontier molecular orbitals of SiNS $Si_{30}H_{48}$ in the (a) ground state geometry and excited state geometries at different simulation time at 50K. Wave function isosurfaces are plotted at the same isovalue (0.013).

When the temperature is increased to 100K, it is bond 1 which has a large enlargement upon excitation (see Figure 3). Hence, the LUMO in S_1 exhibits a distribution mainly localized on bond 1 as shown in Figure 4. The resultant geometry is hence distorted along bond 2, indicating the instability of $Si_{30}H_{48}$ at 100K. Therefore we did not attempt a higher temperature in the MD simulations.
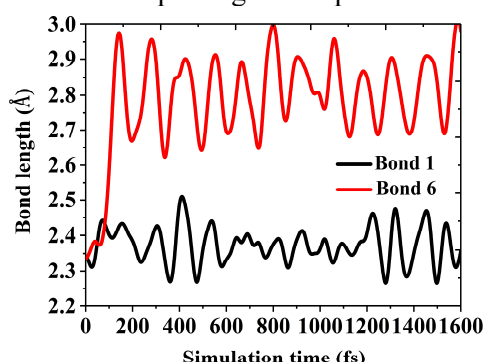

Figure 3. Time evolution of bond length change of labeled bonds at 100K for SiNS $Si_{30}H_{48}$.

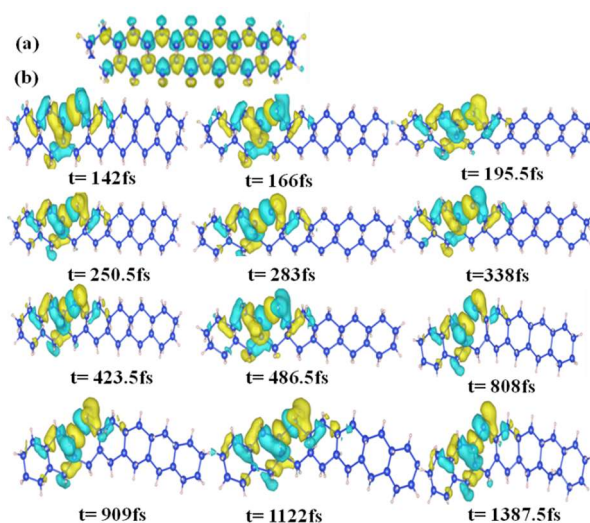**Figure 4**. Frontier molecular orbitals of SiNS $Si_{30}H_{48}$ in the (a) ground state geometry and (b) excited state geometries at different simulation time at 100K. Wave function isosurfaces are plotted at the same isovalue (0.013).

3.2 MD simulation in S_1 for $Si_{60}H_{82}$ at 50K and 100K

By expanding the size of $Si_{30}H_{48}$, excited state MD simulations were also performed for larger structures $Si_{60}H_{82}$ and $Si_{90}H_{112}$. We also examine the time evolution of the critical bond length, and the distribution of molecular orbitals in the S_1 state.

For $Si_{60}H_{82}$, there is also one Si-Si bond becomes enlarged, which could be observed from the snapshots of the MD simulations. The time evolution of bond length change, as shown in Figure 5(b), indicates that bond 1 extends to a value around 2.8 Å. The simulated results have no discrepancies with our previous work [20]. LUMO of the first excited state S_1 still localizes on the Si-Si bond which has a large displacement. When the temperature is increased to 100K, it is bond 4 rather than bond 1 has an obvious enlargement, as shown in Figure 7. At about 780fs, bond 4 exhibits an abrupt decrease in length and bond 1, 2 and 5 become elongated accordingly to conserve the energy. A continuous increase in bond length of bond 4 ensued and hence the trapped exciton has a slight migration to the edge of NSs (see Figure 8).
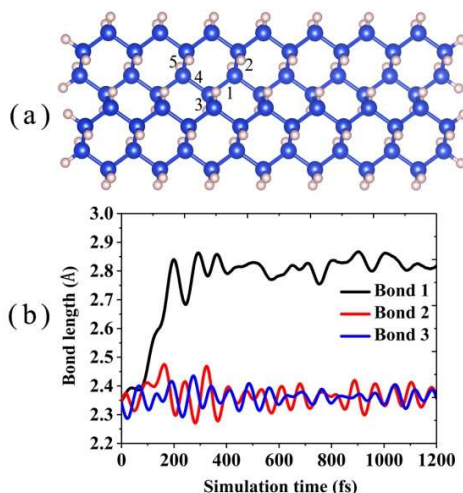

Figure 5. The structures of (a) SiNS $Si_{60}H_{82}$ and (b) time evolution of bond length change of labeled bonds at 50K.
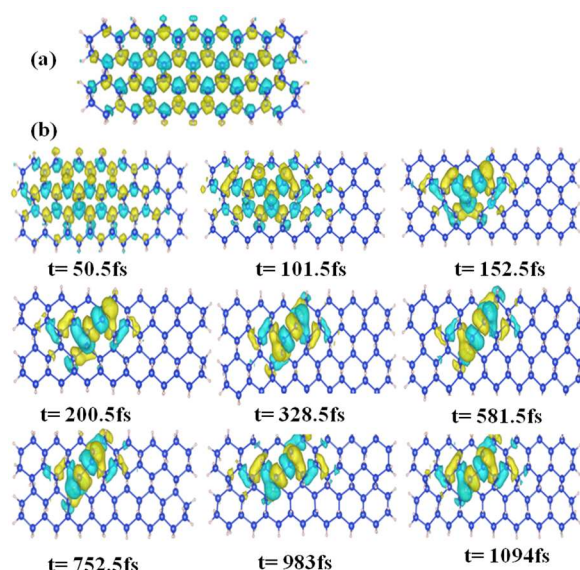
Figure 6. Frontier molecular orbitals of SiNS $Si_{60}H_{82}$ in the (a) ground state geometry and excited state geometries at different simulation time at 50K. Wave function isosurfaces are plotted at the same isovalue (0.013).
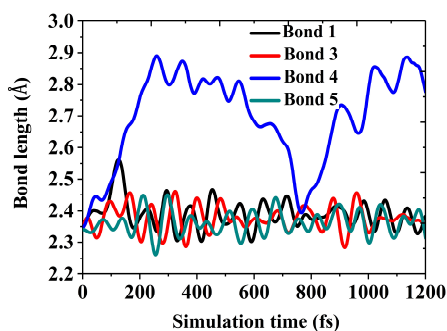

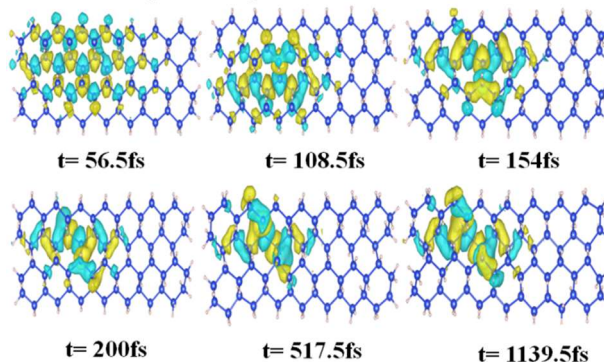**Figure 7**. Time evolution of bond length change of labeled bonds at 50K for SiNS $Si_{60}H_{82}$.

Figure 8. Frontier molecular orbitals of SiNS $Si_{60}H_{82}$ in the (a) ground state geometry and (b) excited state geometries at different simulation time at 100K. Wave function isosurfaces are plotted at the same isovalue (0.013).

3.3 MD simulation in S_1 state for $Si_{90}H_{116}$ at 50K and 100K

In the case of $Si_{90}H_{116}$, the structure distortions of $Si_{90}H_{116}$ distribute on the Si-Si bonds in the vicinity of center, thereby leading to a less deviation from the initial structure. In the initial 200fs in Figure 5.9, it is observed that how the exciton is trapped and localized on certain bonds after the system is excited. With the increase of simulation time, it exhibits a relatively stable distribution of LUMO in S_1.

In the case of $Si_{90}H_{116}$, Si-Si bond 4 as depicted in Figure 9(b) becomes enlarged, which could be observed from the snapshots of the MD simulations. The time evolution of bond length change, as

shown in Figure 9(b), indicates that bond 1 extends to a value around 2.8 Å. While the central Si-Si bond has an average value around 2.35 Å. LUMO of the first excited state still localized on the Si-Si bond which has a large displacement (see Figure 10). In the initial 200fs, the process of exciton trapping on bond 1 is also observed and it finally stabilized on bond 1 and several neighboring bonds with the increase of simulation time. Similarly, the analysis of evolution of bond length change and the frontier molecular orbitals also indicate a localized distribution around bond 4 at 100K (see Figure 11 and 12).

In summary, our MD simulations reveal that the exciton is trapped as a function of the width and temperature. The process of trapping an exciton is observed within the timescale at around 200fs. We also reveal a possible migration of trapped exciton of $Si_{30}H_{48}$, which is helping in finding transport properties more conductive to technological application.
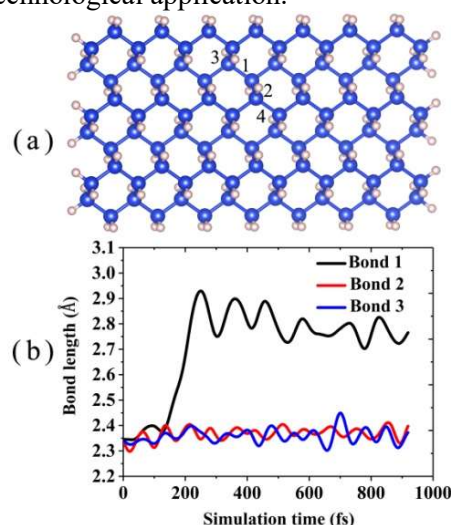

Figure 9. The structures of (a) SiNS $Si_{90}H_{116}$ and (b) time evolution of bond length change of labeled bonds at 50K.
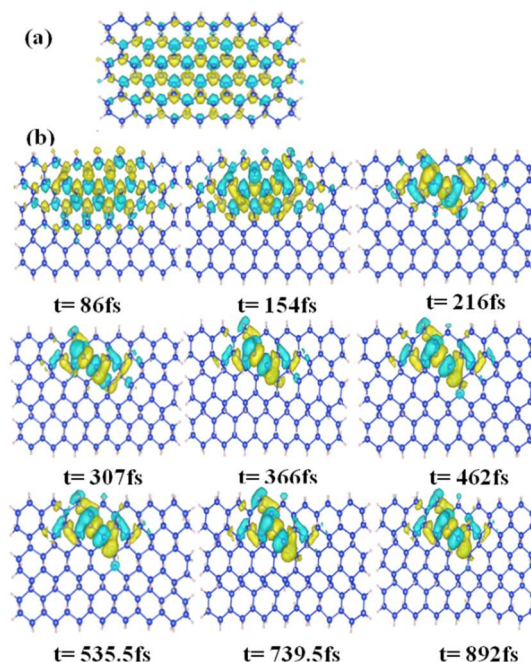

Figure 10. Frontier molecular orbitals of SiNS $Si_{90}H_{116}$ in the (a) ground state geometry and excited state geometries at different simulation time at 50K. Wave function isosurfaces are plotted at the same isovalue (0.013).
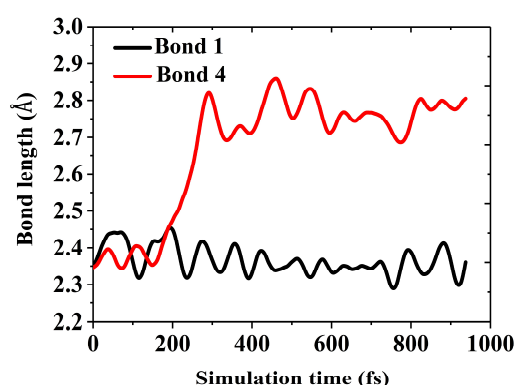
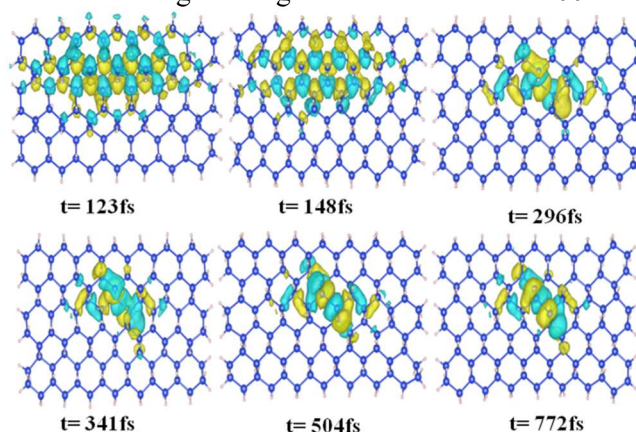**Figure 11**. Time evolution of bond length change of labeled bonds at 100K for SiNS $Si_{90}H_{116}$.

Figure 12. Frontier molecular orbitals of SiNS $Si_{90}H_{116}$ in the (a) ground state geometry and excited state geometries at different simulation time at 100K. Wave function isosurfaces are plotted at the same isovalue (0.013).

4. Conclusions

We have carried our excited state molecular dynamics simulations of silicon nanosheets with finite atomic models, in order to assess the performance of TD-DFTB for the description of excited state relaxation. Our excited state simulation show the relaxation of silicon nanosheets in S_1, which is dominated by a single Si-Si bond. It has a large enlargement in contrast to the initial structure, leading to localization of molecular orbitals on the elongated Si-Si bond. The localized distribution of frontier molecular orbitals and the sufficiently stretched central Si-Si bond signify formation of self-trapping of the exciton in the first excited state. The excited state MD simulations come to a coherent conclusion on the formation of the localized distribution of the frontier molecular orbitals and thus formation of the self-trapped excitons with our previous static investigation. We assert that the TD-DFTB approach proved as a reliable tool in predicting or reproducing the time evolution of excited state structural changes and potential energy surfaces. Since our current TDDFTB molecular dynamics are purely adiabatic, the effect of non-adiabatic coupling between two electronic states will be implemented in the future.

5. References

[1] Weiss U 1999 *Quantum Dissipative Systems* (Singapore: World Scientific)
[2] Klessinger M and Michl J 1995 *Excited States and Organic Molecules* (New York: Wiley-VCH)
[3] Dooley C T, Dore T M, Hanson G T, Jackson W C, Remington S J and Tsien R Y2004 *J. Biol. Chem.* **279** 22284.
[4] Hanson G T, Aggeler R, Oglesbee D, Cannon M, Apaldi R A, Tsien R Yand Remington S J 2004 *J. Biol. Chem*. **279** 13044
[5] Juan Manuel Ortiz-Sánchez, B. Denis, Levi C. T. Pierce, R. L. Phineus, Markwick and J. Andrew Mc Cammon 2012 *J Chem Theory Comput.* **8** 2752–2761
[6] Casida M E 1995 *Recent Advances in Density Functional Methods* (Singapore: World Scientific) Chapter 5 pp 155–192.

[7] Runge E and Gross E K U 1984 *Phys. Rev. Lett*. **52** 997

[8] M. E. Casida 1996 *Theoretical and Computational Chemistry* (Amsterdam: Elsevier) pp 391–439

[9] Porezag D, Frauenheim T, Köhler T, Seifert G and Kaschner R 1995 *Phys. Rev. B* **51** 12947

[10] Seifert G, Porezag D and Frauenheim T 1996 *Int. J. Quantum Chem*. **58** 185

[11] Niehaus T A, Suhai S, Della Sala F, Lugli P, Elstner M G and Frauenheim T 2001 *Phys. Rev. B, 63* 085108

[12] T. A. Niehaus, *J. Mol. Struct.Theochem.* 2009, *914*, 38-49.

[13] Joswig J O, Seifert G, Niehaus T A and Springborg M 2003 *J. Phys. Chem. B* **107** 2897

[14] Frenzel J, Joswig J O and Seifert G 2007 *J. Phys. Chem. C* **111** 10761

[15] Wang X, Zhang R Q, Niehaus T A, and Frauenheim T 2007 *J. Phys. Chem. C* **111** 2394

[16] Wang X, Zhang R Q, Lee S T, Niehaus T A and Frauenheim T 2007 *Appl. Phys. Lett*. **90** 123116

[17] Li Q S, Zhang R Q, Lee S T, Niehaus T A and Frauenheim T 2008 *J. Chem. Phys.* **128** 244714

[18] Zhang R Q, De Sarkar A, Niehaus T A and Frauenheim T 2012 *Phys. Status Solidi B* 249 401

[19] Fan G H , Li X, Liu J Y and He G Z 2012 *Comput. Theor. Chem*. **1030** 17

[20] Wu Q, Wang X H, Niehaus T A and Zhang R Q 2014 *J. Phys. Chem. C* 118 20070-20076

[21 Wu Q, Huang B, Niehaus T, Yang X, Fan J and Zhang R Q 2015 *Phys. Chem. Chem. Phys*. **17** 10786

[22] Heringer D, Niehaus T A, Wanko M and Frauenheim T H 2007 *J. Comp. Chem. 28* 2589-2601

[23] Fehér F 1997 *Molekülspektroskopische Untersuchungen auf dem Gebiet der Silane und der Heterocyclischen Sufane* pp1-55

[24] Yu D K, Zhang R Q and Lee S T 2002 *J. Appl. Phys.* **92** 7453-7458

[25] Lu G H, Huang M, Cuma M and Liu F 2005 *Surf. Sci*. **588** 61-70

[26] Visikovskiy A, Yoshimura M and Ueda K 2010 *Jpn. J. Appl. Phys*. **49** 08LB05

[27] Brázdová V and Bowler D R 2011 *Phys. Chem. Chem. Phys*. **13** 11367-11372

[28] Zheng G, Irle S and Morokuma K 2005 *Chem. Phys. Lett*. **412** 210-216

[29] Sattelmeyer K W, Tirado-Rives T and Jorgensen W L 2006 *J. Phys. Chem. A* **110** 13551–13559

[30] Otte N, Scholten M and Thiel W 2007 *J. Phys. Chem. A* **111** 5751–5755

[31] Goyal P, Elstner M and Cui Q 2011 *J. Phys. Chem B* 2011 **115**, 6790-6805

[32] Domínguez A, Aradi B, Frauenheim T, Lutsker V and Niehaus T A 2013 *J. Chem. Theory. Comput.* **9** 4901-4914

[33] Porezag D, Frauenheim T, Köhler T, Seifert G and Kaschner 1995 *Phys. Rev. B* **51** 12947-12957

[34] Zdetsis A D 2006 *Rev. Adv. Mater. Sci*. **11** 56-78

[35] Meng Y, Wu Q, Chen L, Wangmo S, Gao Y, Wang Z, Zhang R Q and Ding D 2013 *Nanoscale* **5** 12178-12184

Acknowledgments